Planet. Space Sci., Vol. 37, No. 2, pp. 131–143, 1989
Printed in Great Britain.

0032-0633/89 $3.00+0.00

GROUND-BASED OBSERVATIONS OF O_2^+ 1N BAND ENHANCEMENTS RELATIVE TO N_2^+ 1N BAND EMISSION

R. J. NICIEJEWSKI and J. W. MERIWETHER, JR.
Space Physics Research Laboratory, Department of Atmospheric and Oceanic Science, University of Michigan, Ann Arbor, MI 48109-2143, U.S.A.

A. VALLANCE JONES and R. L. GATTINGER
Herzberg Institute of Astrophysics, National Research Council of Canada, Ottawa, Canada K1A OR6

C. E. VALLADARES
Emmanuel College, Boston, MA 02115, U.S.A.

and

V. B. WICKWAR* and J. KELLY
SRI International, Menlo Park, CA 94025, U.S.A.

(*Received* 8 *August* 1988)

Abstract—Spectrometric measurements in normal aurora of O_2^+ first negative (1N) and N_2^+ first negative (1N) emissions over the wavelength range 5175–5325 Å have been obtained with coincident incoherent scatter radar measurements with both instruments pointed in the same direction, the geomagnetic zenith. A comparison of the inferred mean energies derived from the radar observations for several normal aurora was made with the spectral ratio $I(O_2^+$ 1N; 2, 0)/$I(N_2^+$ 1N; 0, 3) obtained from the optical observations. The intensity ratio was found to decrease by nearly 40% from aurora with mean energy ~10 keV to aurora with mean energy ~2 keV. The altitude of the peak *E*-region electron density co-varied with the spectral ratio from ~105 km for the harder aurora to ~130 km for the softer aurora. The inferred rotational temperature from the matching synthetic spectra co-varied from 250 to 500 K over the same energy limits. Model analysis based on both mono-energetic and Maxwellian precipitating electron fluxes show reasonable agreement with the observed $I(O_2^+$ 1N; 2, 0)/$I(N_2^+$ 1N; 0, 3) ratio when MSIS $n(O_2)$ and $n(N_2)$ densities corresponding to the experimental dates are used.

INTRODUCTION

Substantial theoretical studies and experimental measurements of the characteristic energy of the electron flux producing an aurora have shown that the average energy of the precipitating primary electrons associated with the aurora may be estimated from ground-based measurements of spectral ratio of optical emissions in aurora. The N_2^+ 1N (0, 1) band at 4278 Å, the OI (5577 Å), and the OI (6300 Å) emissions are very prominent in aurora, so intensity variations of these emissions are easy to observe. The theoretical study by Rees and Luckey (1974) has shown that the emission rate ratios I(6300 Å)/I(4278 Å) and I(5577 Å)/I(4278 Å) may be used if an assumption is made regarding the form of the primary electron spectra. The form chosen in their study for the incident flux was an isotropic Maxwellian distribution which is characteristic of the stable diffuse aurora.

The I(6300 Å)/I(4278 Å) spectral ratio has been widely used to infer the mean energy (twice the characteristic, or peak energy of a Maxwellian distribution) of the precipitating electrons in an aurora (Eather *et al.*, 1976; Arnoldy and Lewis, 1977; Vondrak and Sears, 1978; Mende *et al.*, 1984; Christensen *et al.*, 1987; Vallance Jones *et al.*, 1987; Niciejewski and Forsyth, 1988). The I(5577 Å)/I(4278 Å) spectral ratio has also been used, particularly in inferring mean energies of pulsating auroras (Sawchuk and Anger, 1976; McEwen and Bryant, 1978; McEwan *et al.*, 1981). However, this ratio is not as sensitive to variations in energy and there are difficulties in explaining the chemistry dependence of the OI (5577 Å) emission.

Recently, Hecht *et al.* (1985) have shown that the OI (8446 Å) multiplet observed in aurora is excited by electron impact on atomic oxygen indicating that the ratio I(8446 Å)/I(4278 Å) should be directly related to the [O]/[N_2] ratio, which varies considerably over the height range of aurora. Observations of these two

* Now at CASS, Utah State University, Logan, UT 84322, U.S.A.

emissions by Vallance Jones *et al.* (1987) show that there is a good correlation between the average energy of the precipitating electrons and this spectral ratio.

The comparison of intensities of molecular oxygen and molecular nitrogen emissions has been made for normal and type-B red aurora (Hunten, 1955; Rodulgin, 1968; Shemansky and Vallance Jones, 1968; Gattinger and Vallance Jones, 1979; Lummerzheim, 1987). Type-B aurora is characterized by a distinct red lower border, with a typical height between 80 and 100 km. These results show that the intensities of the O_2^+ 1N system are enhanced relative to both the N_2^+ 1N and the N_2 1PG systems. Also found was a decrease in the $I(O_2^+ 1N; 2,0+3,1)/I(N_2^+ 1N; 0,3)$ spectral ratio of 16% from the lower altitude type-B aurora to the higher altitude normal aurora. Since it is generally accepted that both the O_2^+ 1N and N_2^+ 1N band systems are excited by electron impact on O_2 and N_2, respectively, the spectral ratio is proportional to the $[O_2]/[N_2]$ number density ratio which is height dependent. Henriksen *et al.* (1987) outlined a method to obtain neutral temperatures and height changes in the aurora using the O_2^+ 1N and N_2^+ 1N systems.

The observations reported in this work were obtained during a CEDAR (Coupling, Energetics, and Dynamics of the Atmospheric Regions) campaign in Søndre Strømfjord, Greenland, during a new moon period in February/March 1987. The campaign has been described by Niciejewski *et al.* (1989). Optical observations were performed in coordination with the Søndre Strømfjord incoherent scatter radar. The goal was to compare changes in the spectral ratio with changes in the average primary electron energy, the latter determined by the radar measurements. The radar data also provided independent measurements of the altitude of the aurora. The results show that the spectral ratio $I(O_2^+ 1N; 2,0)/I(N_2^+ 1N; 0,3)$ decreased by nearly 40% when the average energy of the precipitating electrons in the aurora varied from 10 to 2 keV.

INSTRUMENTATION

The spectrometric observations were obtained with a 0.5 m Ebert–Fastie spectrometer in a photon counting mode. This instrument has been described by Vallance Jones and Gattinger (1972) and Gattinger and Vallance Jones (1974). In Søndre Strømfjord, the spectrometer was used in a programmable scanning mode as described in Niciejewski *et al.* (1989). During auroral displays, the instrument acquired spectra over the wavelength range 5175–5325 Å out of the total possible range, in first order, of 4000 Å. The instrumental profile was triangular with a spectral width of 8 Å. Spectra were acquired in 30 s at one sample per 1.9 Å. Variations in the wavelength sensitivity of the spectrometer were removed with the aid of a low brightness source calibration. This source has been compared against a standard source at the National Research Council of Canada in Ottawa and should have a relative error of less than 10% over the spectral region scanned (Gattinger and Vallance Jones, 1974). A set of spectral lamps provided the wavelength calibration. The spectrometer was pointed in the geomagnetic zenith direction to match the pointing of the incoherent scatter radar. The spectrometer had a field of view of 4°.

A filter photometer, pointing in the same direction as the spectrometer, monitored the N_2^+ 1N (0, 1) band emissions at 4278 Å so that the spectrometer observations could be corrected for auroral fluctuations. The photometer had the same field of view as the spectrometer.

The Søndre Strømfjord incoherent scatter radar acquired electron density height profiles of the *E*- and lower *F*-regions in the geomagnetic zenith direction with a temporal resolution of 15 s. Details regarding the radar's setup and operation are given in Niciejewski *et al.* (1989).

OBSERVATIONS

Coordinated optical–radar measurements for this study were achieved on four of the nine nights of the campaign. Electron number density profiles derived from the radar measurements were analyzed using the UNTANGLE technique (Vondrak and Baron, 1976) to determine the energy flux and the mean energy of the precipitating electrons associated with the aurora. An MSIS-86 neutral atmosphere model appropriate for the observing conditions was used in the analysis rather than the default model that is normally used with UNTANGLE. The peak energy flux derived was 46.8 ergs cm^{-2} s^{-1}, while the highest mean energy obtained was 10.5 keV. The lowest altitude of the peak electron number density was 104 km, indicating normal type aurora. In this study, we report results from bright auroral events that occurred during the dates 59 (28 February 1987) and 63 (4 March 1987). The derived electron energy fluxes and the mean energies for these two dates are shown in Fig. 1. The periods of energetic auroral display occurred at 00:30 and 01:55 U.T. on day 59 and 01:00 and 04:05 U.T. on day 63. Additional weaker events were interspersed throughout the nights.

For these two nights of the coordination, the optical data were sorted into bins 1 keV wide based on the

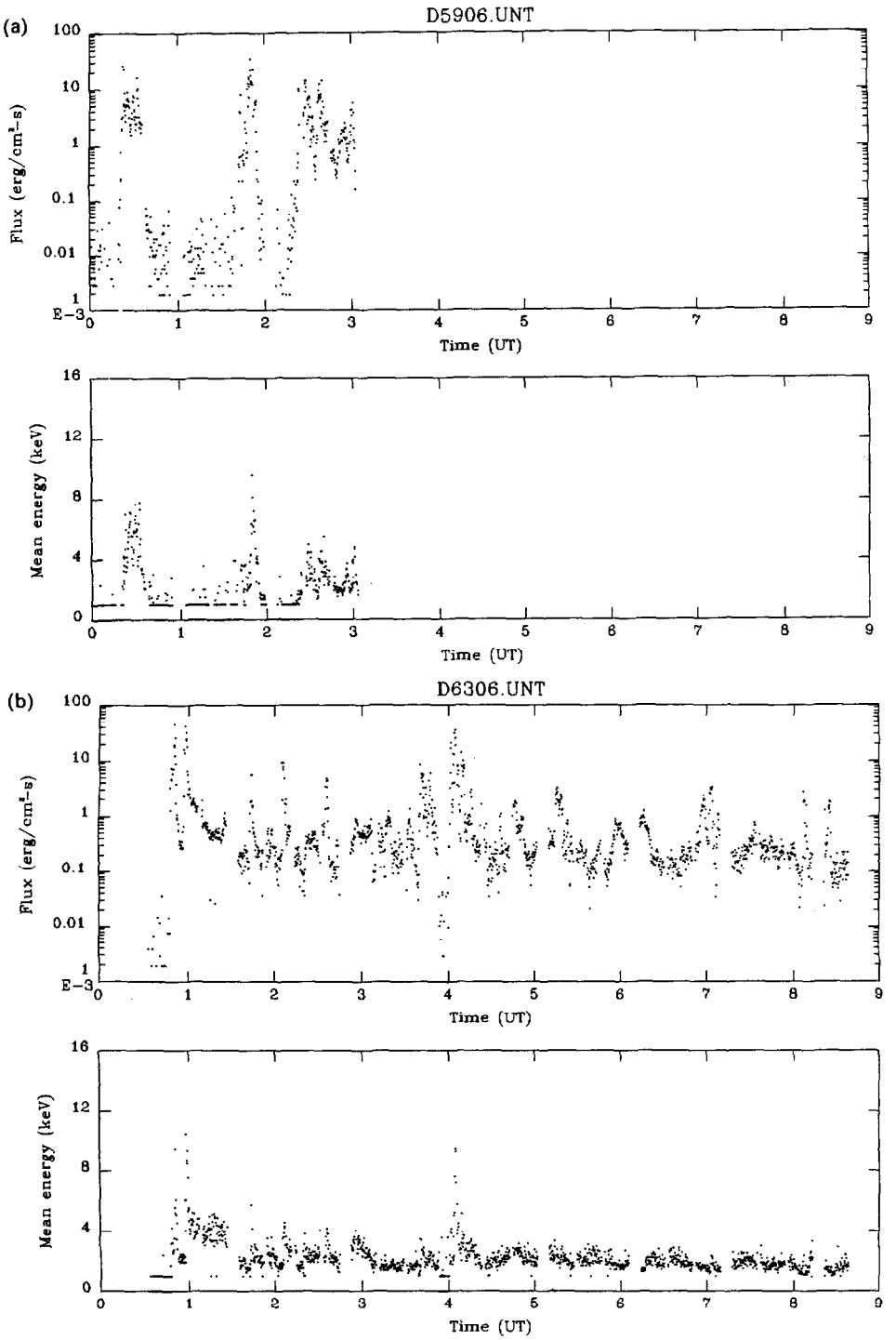

FIG. 1(a) ELECTRON ENERGY FLUX AND MEAN ELECTRON ENERGY DERIVED FROM INCOHERENT SCATTER RADAR OBSERVATIONS IN THE GEOMAGNETIC ZENITH ON 28 FEBRUARY 1987.
Values are shown at 15 s resolution. (b) The same for 4 March 1987.

corresponding mean energy. The only spectra selected were those for which the electron energy flux was greater than 1 erg cm^{-2} s^{-1} and the mean electron energy was greater than 2 keV. The number of spectra passing through this filter was 127. Some of the lesser populated higher energy bins were co-added to increase the signal to noise ratio of the spectra in those bins. Two examples of the final co-added spectra are shown in Fig. 2. Each spectra has been corrected for brightness fluctuations in the aurora by normalizing with simultaneous I(4278 Å) monitor photometer measurements. The wavelength intensity dependence of the spectrometer has also been removed. However, correction for atmospheric attenuation was not made. It was not necessary to correct the emissions to the zenith since the optical measurements were acquired within 10° of the overhead point.

MODELLING

Synthetic spectra were constructed for both the O_2^+ 1N (2, 0) and (3, 1) bands and the N_2^+ 1N (0, 3) band emissions using the technique described in Vallance Jones and Gattinger (1972) and Gattinger and Vallance Jones (1974). Updated Hönl–London line strength factors (Henriksen and Veseth, 1987) for all 48 branches of the O_2^+ 1N emission were incorporated as a part of the application of this synthetic fitting routine. The temperature dependence for each of the three bands within the scan range is shown in Fig. 3. Here, the synthetic spectra are shown convolved with the instrumental profile for six different temperatures ranging from 150 to 650 K in steps of 100 K. The N_2^+ 1N (0, 3) band exhibits a more pronounced blueward tail as temperature increases, but retains the rapid decrease in intensity at the redward limit. The two bands synthesized for O_2^+ 1N are quite similar in appearance. As temperature increases, each shows variations in their convolved envelopes.

The observed spectra were fitted with a multiple linear regression analysis technique with seven variables: the three band emission intensities, the atomic line emission intensity, the background level, wavelength, and temperature. The individual rotational lines of the synthetic spectra were convolved with the instrumental profile and the final spectra were generated at 0.1 Å spacing. Spectra were synthesized for the temperature range 150–650 K at 25 K intervals. Final temperatures were determined by searching for the best fit between an observed spectra and the set of synthetic spectra in the least squares sense.

The fit between observed and synthetic spectra is demonstrated in the series of plots for 28 February 1987, in Fig. 4. The fit is generally quite good for all the averaged spectra. Only the (2, 0) and the (3, 1) bands of O_2^+ 1N have been included, since the contribution of the (4, 2) band was shown to be negligible. The temperature fit varied as expected: the lower the mean energy, the higher the temperature. The NI (5200 Å) doublet feature was fitted by using the instrumental transmission function adjusted to match the intensity ratio of the observed emission. The resolution of the spectrometer was insufficient to resolve the NI doublet, since the two components are only 2 Å apart.

The observed spectral ratios may be compared with values calculated from a model of the neutral atmospheric composition and theoretical ionization rate height profiles calculated by the procedure first described by Rees (1963). The version used in this study has been described by Vallance Jones (1975) and follows the Rees approach. From the ionization rate profile one may derive values for the production rates of O_2^+ and N_2^+ ions and from these the emission rates of the bands observed.

The total ionization rate profile was calculated as described in detail in Vallance Jones (1974). The ionization rate of N_2 was then calculated from equation (4.2.1f) in the same reference. Finally, the emission rate of the (0, 0) band of the first negative system of N_2^+ is given by the relation

$$\eta(N_2^+ B^2\Sigma; 0, 0) = (0.093) \times (0.76)\eta_i(N_2), \quad (1)$$

according to the branching ratios given in the reference.

The emission rate for the (1, 0) O_2^+ band of the first negative system may be related to that of the (0, 0) N_2^+ first negative band by means of the laboratory measurements of the cross-sections for the excitation of these bands which were measured in a self-consistent way by Borst and Zipf (1970a,b). Because the cross-sections are very similar in shape and peak energy, one may assume, to a good approximation, that the volume excitation rates for the bands are proportional to the product of the peak excitation cross-section and the concentration of the target molecules. The relevant cross-sections are given in Table 1.

TABLE 1. EXCITATION CROSS-SECTIONS USED IN THE MODELLING

Species	Emission band	Maximum cross-section (cm^2)	Reference
O_2	(1, 0)	4.33×10^{-18}	Borst and Zipf (1970a)
N_2	(0, 0)	17.4×10^{-18}	Borst and Zipf (1970b)

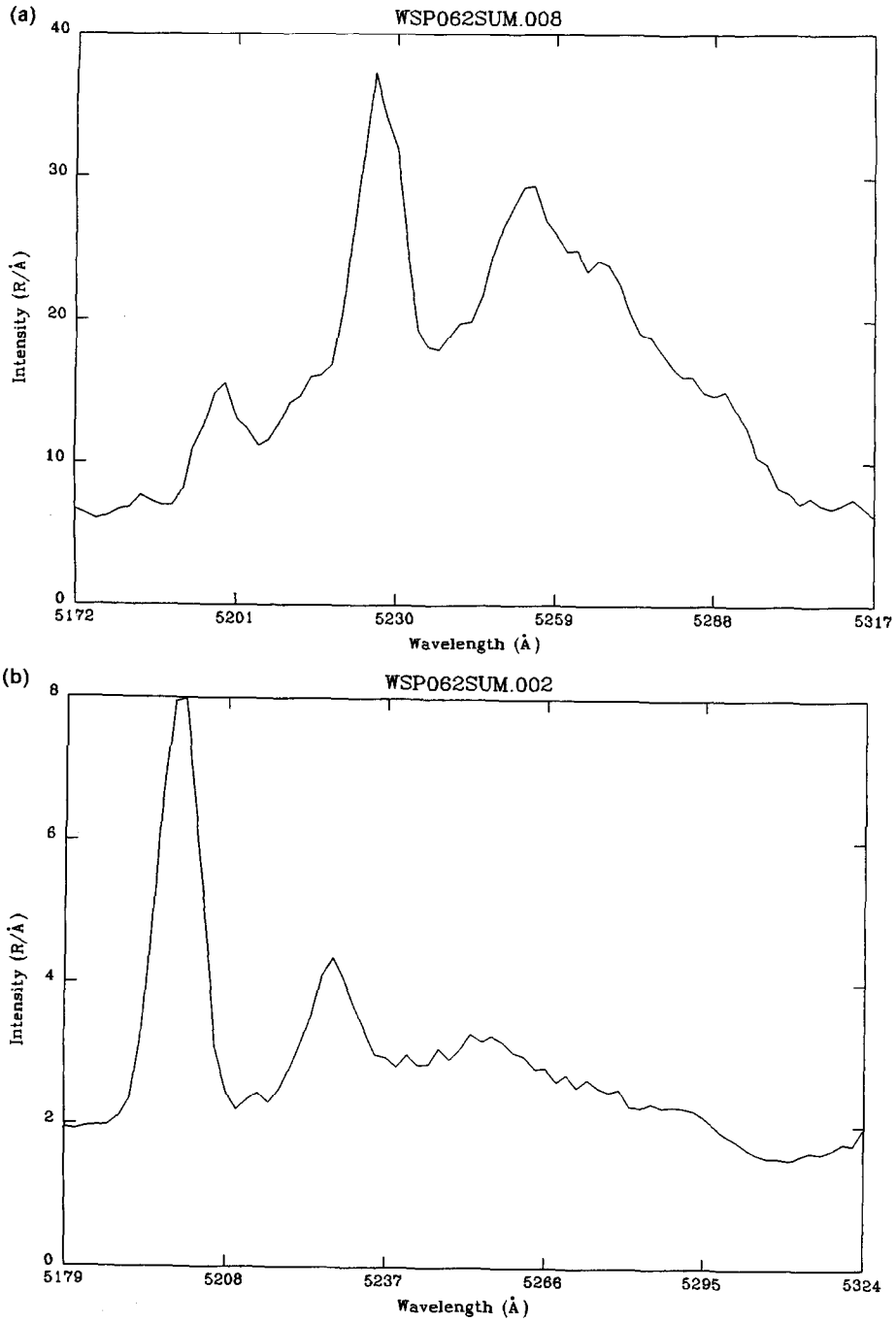

FIG. 2(a) CO-ADDED SPECTRUM CORRESPONDING TO THE ENERGY BIN 8–12 keV FOR 4 MARCH 1987. The spectrum has been corrected according to the test. (b) The same for the energy bin 2–3 keV for 4 March 1987.

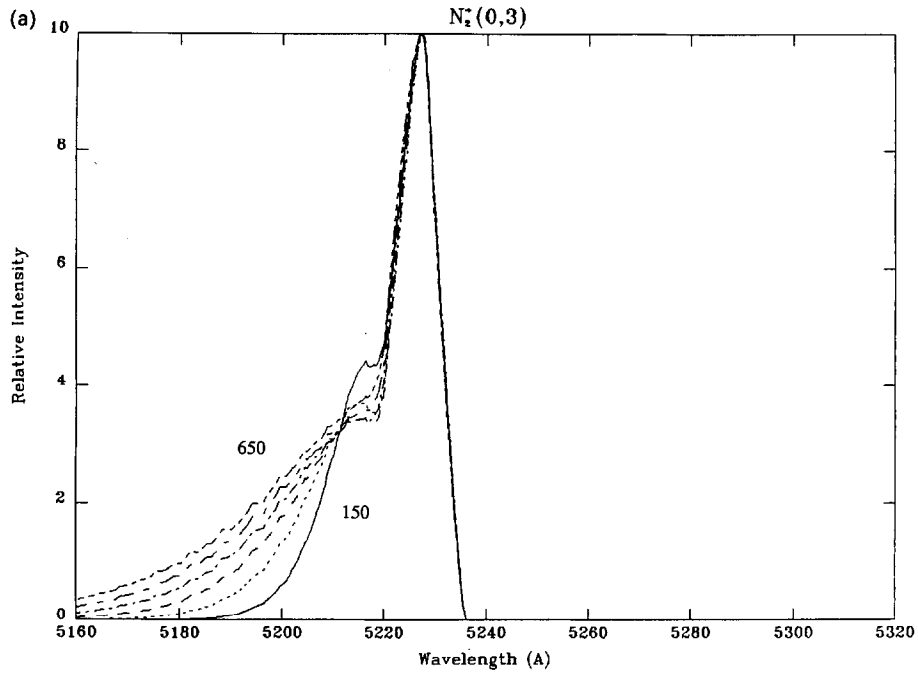

FIG. 3(a)—Caption overleaf.

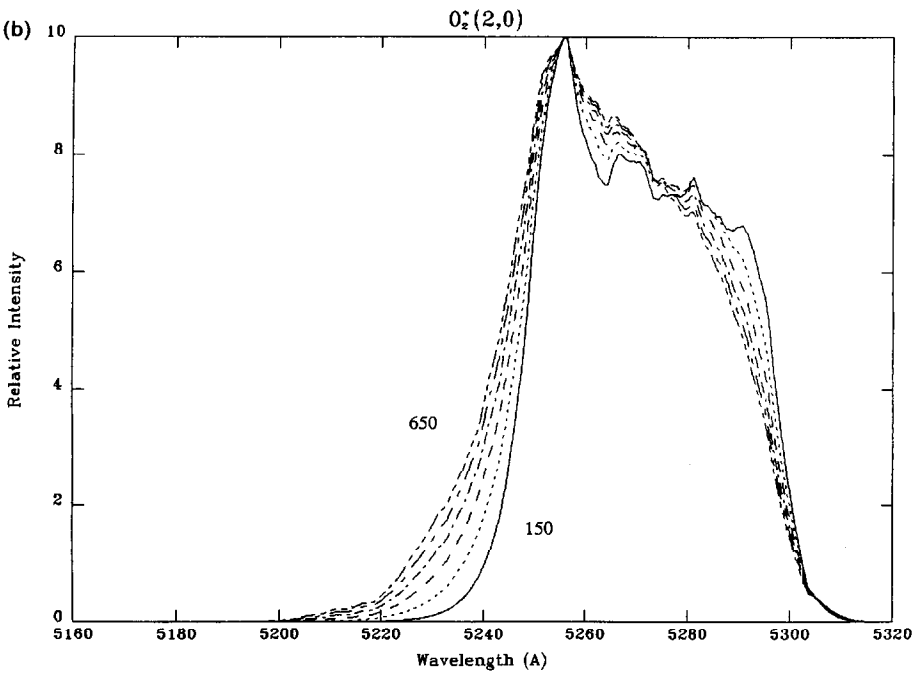

FIG. 3(b)—Caption overleaf.

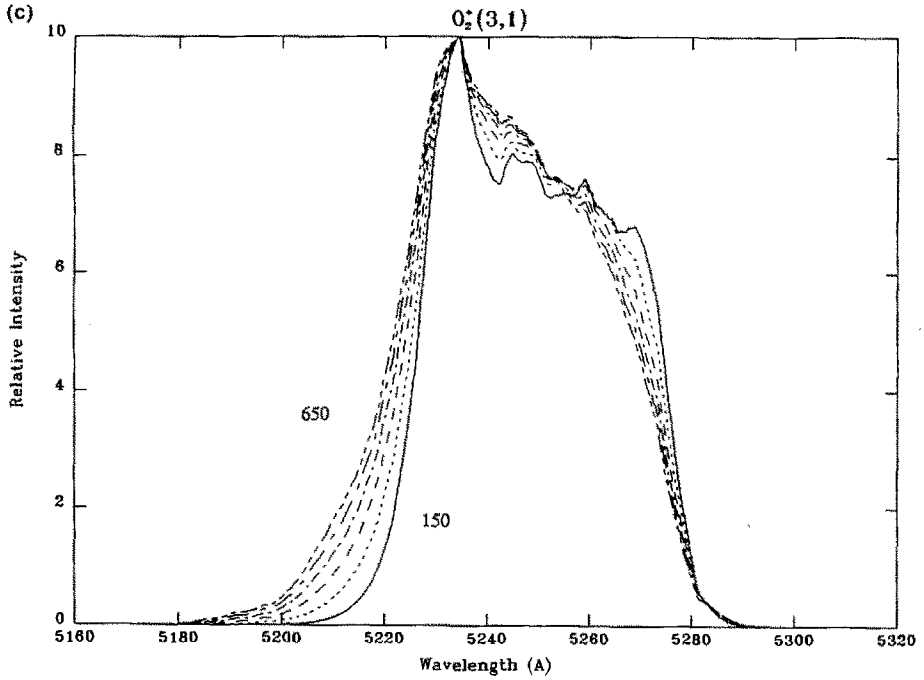

FIG. 3(a) TEMPERATURE DEPENDENCE OF THE N_2^+ 1N (0, 3) BAND.
The temperature range is 150–650 K in steps of 100 K. (b) The same for the O_2^+ 1N (2, 0) band. (c) The same for the O_2^+ 1N (3, 1) band.

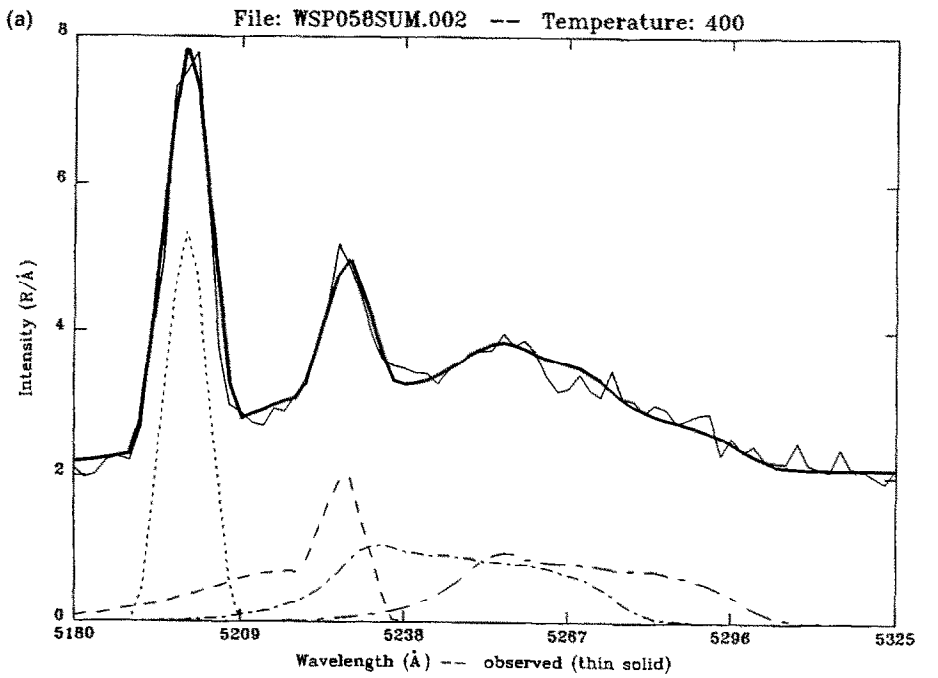

FIG. 4(a)—Caption on p. 139.

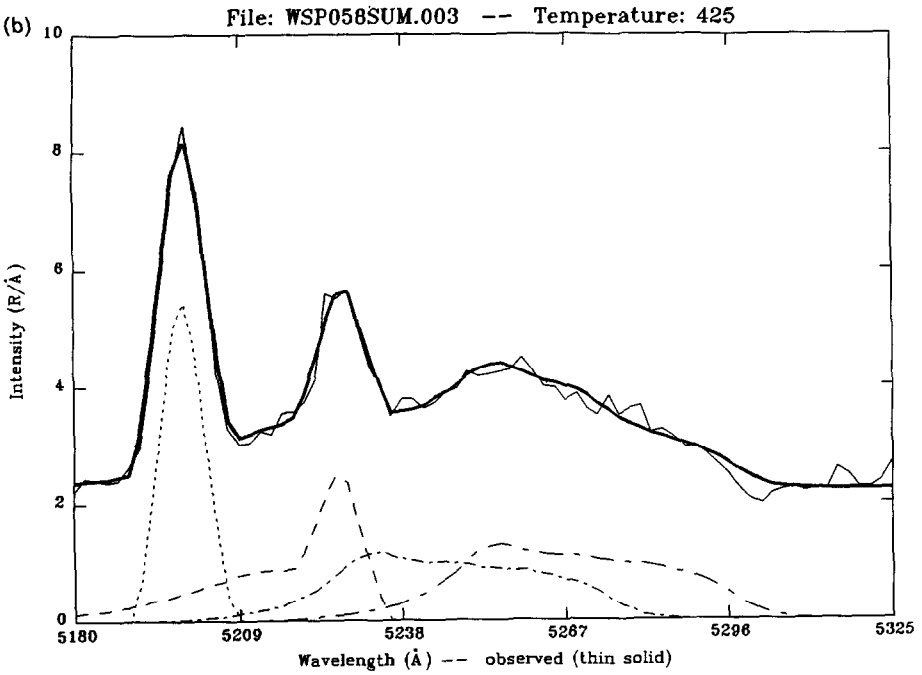

FIG. 4(b)—Caption on p. 139.

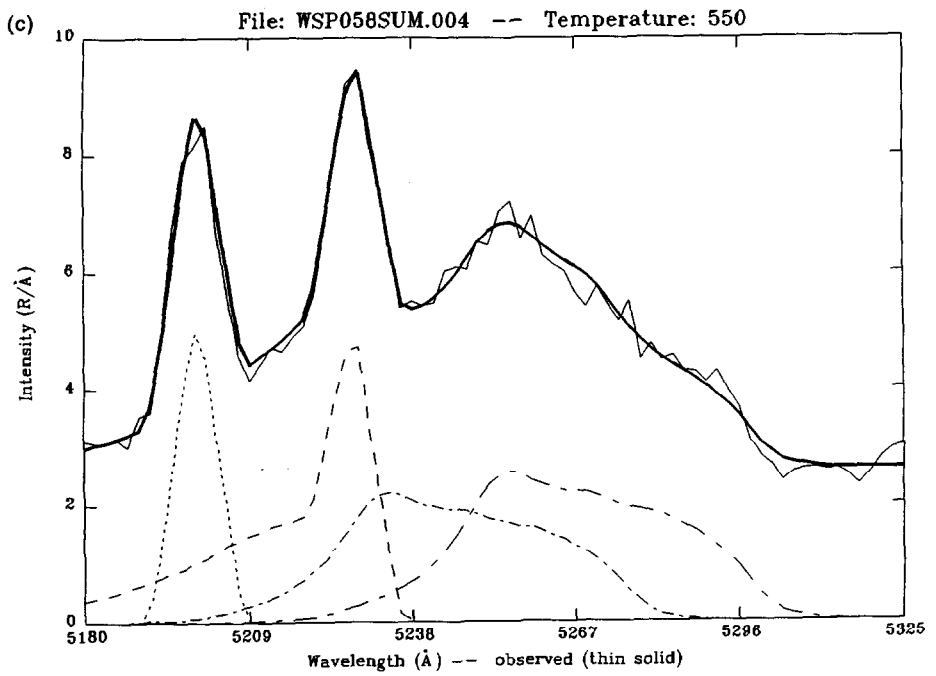

FIG. 4(c)—Caption on p. 139.

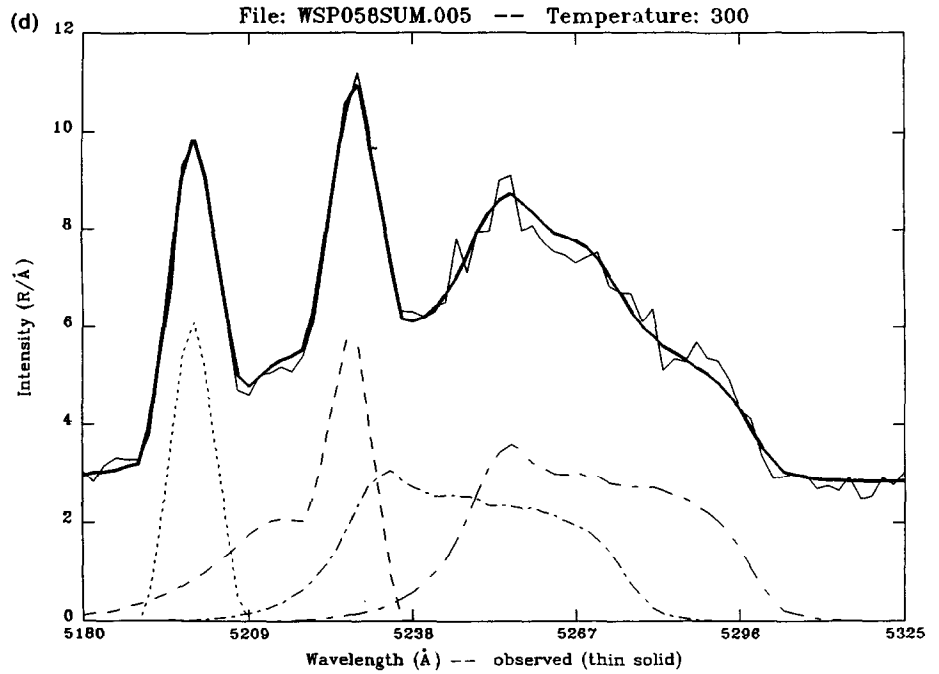

FIG. 4(d)—Caption on p. 139.

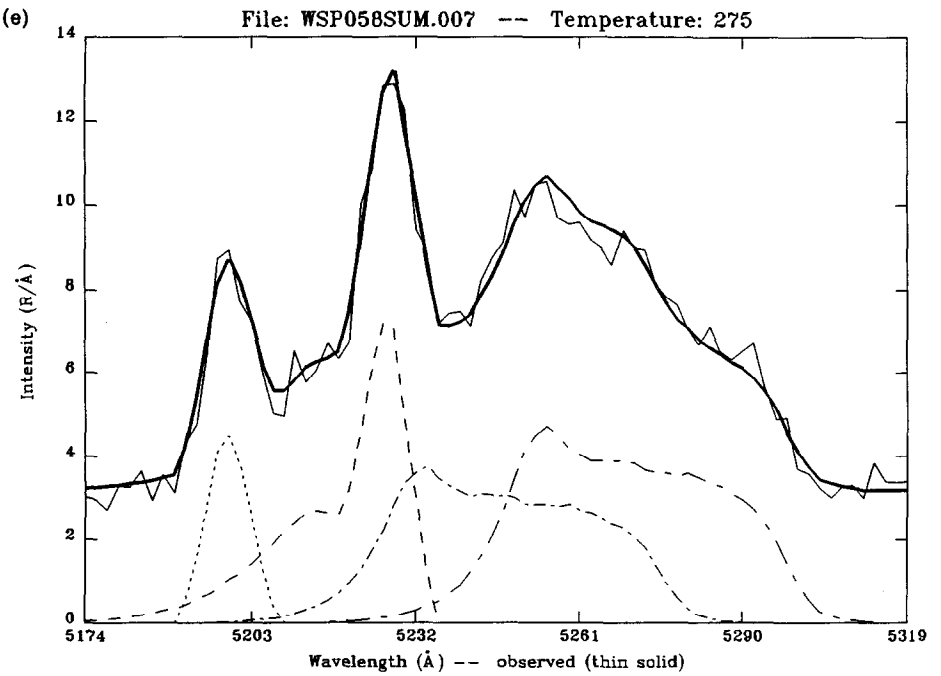

FIG. 4. OBSERVED (THIN SOLID LINE) AND FINAL FITTED (THICK SOLID LINE) SPECTRA FOR THE SET OF SPECTRA FOR 28 FEBRUARY 1987.

Along the bottom of each plot the contributions to the final synthetic spectrum are indicated. From lowest to highest wavelengths, the synthetic components correspond to NI (5200 Å), N_2^+ 1N (0, 3), O_2^+ 1N (3, 1) and O_2^+ 1N (2, 0). Shown are the final fits for energy bin (a) 2–3 keV (temperature: 400 K), (b) 3–4 keV (425 K), (c) 4–5 keV (550 K), (d) 5–7 keV (300 K) and (e) 7–8 (275 K).

Consequently, the total intensity of the O_2^+ 1N (1, 0) band is given by the relation,

$$\eta(O_2^+ b^4\Sigma; 1, 0) \approx 0.25\eta(N_2^+ B^2\Sigma; 0, 0) \times [n(O_2)/n(N_2)]. \quad (2)$$

The relative intensities of the (0, 3) and (0, 0) vibrational bands for the N_2^+ first negative system depend only on the band transition probabilities and are in the ratio 0.99/98.5 (Vallance Jones, 1974) while the relative intensities of the (2, 0) and (1, 0) O_2^+ bands of the first negative system have been measured to be in the ratio 1.80/5.94 by Gattinger and Vallance Jones (1974).

Finally the volume emission rates for the bands of interest are given by the relations,

$$\eta(O_2^+ b^4\Sigma; 2, 0) = 0.0758[n(O_2)/n(N_2)] \times \eta(N_2^+ B^2\Sigma; 0, 0) \quad (3)$$

and

$$\eta(N_2^+ B^2\Sigma; 0, 3) = 0.010\eta(N_2^+ B^2\Sigma; 0, 0). \quad (4)$$

The predicted zenith intensity ratios are obtained from the height integrals of these volume emission rates.

The predictions were performed with the MSIS-86 model atmosphere with the same input parameters as used for the UNTANGLE calculations. A range of monoenergetic and Maxwellian primary electron fluxes with a downward isotropic angular distribution was considered. The predicted spectral ratio is tabulated in Table 2 along with MSIS-86 predictions for $n(O_2)$, $n(N_2)$, and neutral temperature for 120 km. The exospheric temperature is also listed.

Table 3 presents the fitted NI (5200 Å) intensity, N_2^+ 1N (0, 3), O_2^+ 1N (3, 1) and (2, 0) band intensities, and the spectral ratio $I(O_2^+ 1N; 2, 0)/I(N_2^+ 1N; 0, 3)$ for the indicated energy bins. Over the mean energy range studied, the spectral ratio varies from 1.05 to 1.76. Figure 5 shows the correspondence between the predicted and the fitted ratios. The standard deviation of the fitted ratio is indicated by the vertical bars. The discrete values of the observed spectral ratio

TABLE 2. PREDICTED $I(O_2^+ 1N; 2, 0)/I(N_2^+ 1N; 0, 3)$ SPECTRAL RATIO FOR MONOENERGETIC FLUXES AND MAXWELLIAN FLUXES OF VARIOUS ENERGIES.

The energy $\langle E \rangle$ refers to the mean electron energy in the Maxwellian electron flux calculations. Also listed are density and temperature parameters generated by the MSIS-86 model for the observing conditions on 4 March 1987, Søndre Strømfjord

	$\langle E \rangle$ (keV)	$\frac{I(O_2^+ 1N; 2, 0)}{I(N_2^+ 1N; 0, 3)}$
Monoenergetic flux		
	1.00	0.96
	2.15	1.13
	5.62	1.43
	10.0	1.61
	14.7	1.69
Maxwellian flux		
	1.02	0.98
	3.01	1.26
	6.04	1.47
	10.0	1.61
	13.9	1.71

$n(O_2)$ at 120 km	0.53×10^{11} cm^{-3}
$n(N_2)$ at 120 km	0.28×10^{12} cm^{-3}
Temperature at 120 km	372 K
Exospheric temperature	816 K

TABLE 3. FITTED INTENSITIES OF SPECTRAL FEATURES AND ASSOCIATED MEAN ENERGIES.

Energy bin indicates the radar derived mean energy limits used in the spectra co-addition process. The tabulated $\langle E \rangle$ is the average of the mean energies in each bin

Date (1987)	Energy bin (keV)	Number of spectra in bin	NI (5200 Å) (R)	N_2^+ 1N (0, 3) (R)	O_2^+ 1N (3, 1 + 2, 0) (R)	$\frac{I(O_2^+ 1N; 2, 0)}{I(N_2^+ 1N; 0, 3)}$	$\langle E \rangle$ (keV)
28 February							
	2–3	17	49	35	47 42	1.18	2.5
	3–4	15	50	45	51 57	1.28	3.5
	4–5	14	45	91	99 117	1.29	4.5
	5–7	9	56	99	131 155	1.57	6.2
	7–8	3	42	123	158 202	1.64	7.5
4 March							
	2–3	28	55	32	43 34	1.05	2.5
	3–4	19	49	50	78 61	1.21	3.5
	4–5	13	63	51	60 65	1.26	4.5
	5–8	5	70	135	192 237	1.76	6.5
	8–11	4	51	365	499 556	1.52	9.5

follow the trend suggested by the auroral excitation/ionization model very well. The difference between monoenergetic and Maxwellian type primary fluxes is slight.

DISCUSSION

Figure 5 shows that the spectral ratio $I(O_2^+ 1N)/I(N_2^+ 1N)$ is sensitive to the energy of the precipitating electrons in the energy range 2–10 keV. The mean primary electron energies have been determined independently by the Søndre Strømfjord incoherent scatter radar. The variation of the ratio over a range of energies indicates that this spectral ratio can supplement other spectral ratios in inferring the mean energy of the electrons associated with an auroral form. The $I(6300\ Å)/I(4278\ Å)$ spectral ratio is generally believed to be a good indicator of the mean energy of soft aurora providing a measure for energies less than 2 keV.

The fact that the neutral atmosphere above the turbopause is in a state of diffusive equilibrium implies that the $n(O_2)/n(N_2)$ density ratio will be dependent on altitude and will decrease with increasing height. The spectral ratio $I(O_2^+ 1N)/I(N_2^+ 1N)$ will then also be height dependent, since each molecular state is generally believed to be produced only by electron impact ionization. There should then be an upper limit to this spectral ratio, determined by the altitude of the turbopause below which mixing should dominate. If the MSIS-86 model is a reasonable representation of the neutral atmosphere, then the predicted spectral ratio does have an asymptotic appearance at higher mean electron energies (lower altitudes of penetration). This implies that this spectral ratio would not be a very good indicator of the mean energy of very hard precipitating electrons, but that it should be satisfactory for all other energies.

The close agreement between the observed and the predicted intensity spectral ratio may be attributed to the care that was taken to ensure that many of the uncertainties were minimized and to the fact that the radar measurements provided a good indication of the aurora's height and energy spectral distribution.

All spectrometer measurements were obtained with coincident N_2^+ 1N (4278 Å) filter photometer measurements with fields of view that were identical and

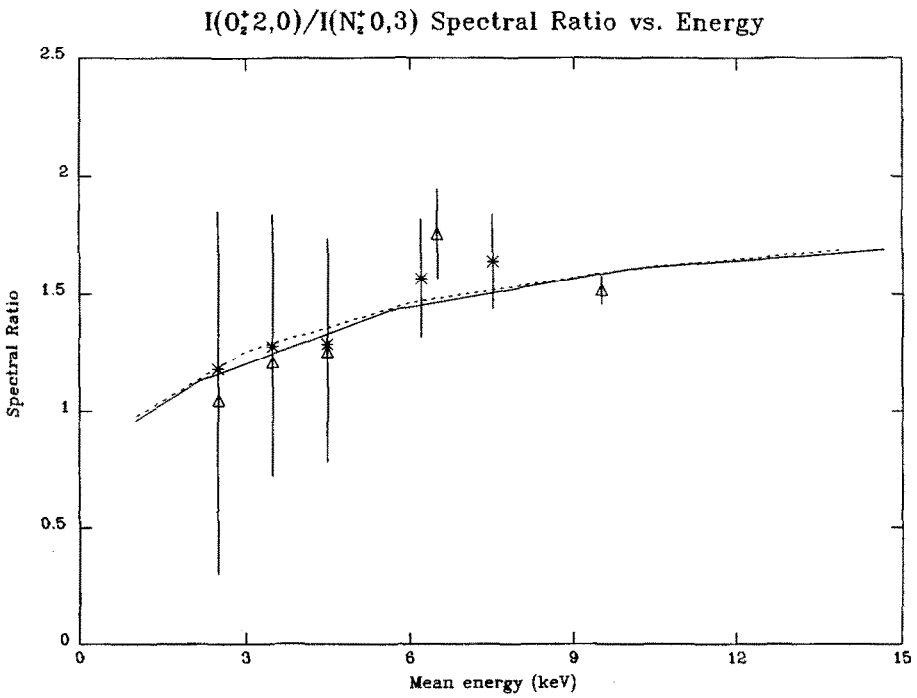

FIG. 5. OBSERVED AND THEORETICAL $i(O_2^+ 1N; 2,0)/I(N_2^+ 1N; 0,3)$ SPECTRAL RATIO AS A FUNCTION OF MEAN PRIMARY ELECTRON ENERGY.
The points for 28 February are indicated with a (*) and the points for 4 March with a (Δ). Standard deviations from the multiple linear regression fit are also indicated. The predicted monoenergetic flux ratio is indicated with a solid line, and the predicted Maxwellian flux ratio is shown with the dashed line.

matched to point at the same emission column at the same temporal resolution. This ensured that any intensity fluctuations in the spectrometric data could be normalized to intensity fluctuations in the photometric data for the prompt band emissions. In addition, the closeness in wavelength of the two emission bands makes atmospheric extinction corrections in the spectral ratio insignificant.

The UNTANGLE algorithm is an empirical technique that assumes that the observed electron density profile may be approximated by a sum of density profiles associated with precipitating monoenergetic electron beams. These individual profiles are chosen from a library of 16 ionization production profiles that have been calculated for energies from 1 to 150 keV. The model requires a neutral atmosphere profile to calculate the range of the precipitating electrons, and this was provided by an MSIS-86 calculation for the period studied. Since there is a lower energy limit in the applicability of the UNTANGLE method, the spectroscopic data base was screened to exclude all spectra that corresponded to low mean electron energies.

The spectra were co-added to reduce the statistical error involved in fitting to synthetic spectra. The spectra were assigned a mean energy and then were added into bins of width 1 keV. Thus, the final spectra were smeared in terms of mean energy. Refining the energy calculations would not add much to the final results.

The actual fitting was accomplished with a computer algorithm based on a multiple linear regression technique. Final intensities were determined by searching for the smallest error in a comparison with the library of synthetic spectra. Wavelength and background were left variable and were determined by the best fit.

The MSIS-86 model was chosen to represent the neutral atmosphere because it is the most recent in the series and does include experimental data on O_2 for the height range considered. However, this implies that the composition is fixed with regard to the $n(O_2)/n(N_2)$ density ratio.

The theoretical result depends on several different measured cross-sections and observed band intensity ratios involved in the transition from the ionization rates of N_2^+ and O_2^+ which are the real products of theory. There is little that can be done to improve this situation, other than using the currently accepted values.

In future auroral studies, the best way to monitor the $I(O_2^+\ 1N)/I(N_2^+\ 1N)$ spectral ratio is to perform the measurement with a multi-channel filter photometer system. Many sites routinely monitor the N_2^+ 1N emission at 4278 Å, so these sites would require only one additional filter to generate on $I(O_2^+\ 1N)/I(N_2^+\ 1N)$ spectral ratio. Preferably, the emissions monitored should be closer together in wavelength so that the atmospheric extinction corrections required for each component of the spectral ratio are similar to each other. For this reason, it would be better to monitor the N_2^+ 1N (0, 2) feature at 4709 Å rather than the (0, 1) emission. The (0, 2) band emission rate is also six times as great as the (0, 3) band. A filter photometer measurement of the (0, 3) band is difficult because of the O_2^+ 1N contamination, which was not a problem in the current spectrometric study. The filter for the O_2^+ 1N emission should be centered near 5260 Å with a bandwidth of 30 Å. This would monitor both the (3, 1) and the (2, 0) band emissions and would discriminate against N_2^+ 1N (0, 3) radiation.

Acknowledgements—We wish to acknowledge the indispensable help of the site crew of the Sondrestrom Radar Laboratory for sustaining the large number of us who were present for the CEDAR campaign. This work was supported by NSF grant ATM-8419806.

REFERENCES

Arnoldy, R. L. and Lewis, P. B., Jr. (1977) Correlation of ground-based and topside photometric observations with auroral electron spectra measurements at rocket altitudes. *J. geophys. Res.* **82**, 5563.

Borst, W. L. and Zipf, E. C. (1970a) Excitation of O_2^+ 1N bands by electron impact on O_2. *Phys. Rev.* **A5**, 1410.

Borst, W. L. and Zipf, E. C. (1970b) Cross-section for *e* impact excitation of the 0, 0 1N N_2^+ band from threshold to 3 keV. *Phys. Rev.* **A1**, 834.

Christensen, A. B., Lyons, L. R., Hech, J. H., Sivjee, G. G., Meier, R. R. and Strickland, D. G. (1987) Magnetic field-aligned electric field acceleration and the characteristics of the optical aurora. *J. geophys. Res.* **92**, 6163.

Eather, R. H., Mende, S. B. and Judge, R. J. R. (1976) Plasma injection at synchronous orbit and spatial and temporal auroral morphology. *J. geophys. Res.* **81**, 2805.

Gattinger, R. L. and Vallance Jones, A. (1974) Quantitative spectroscopy of the aurora. II—The spectrum of medium intensity aurora between 4500 and 8900 Å. *Can. J. Phys.* **52**, 2343.

Gattinger, R. L. and Vallance Jones, A. (1979) Observations and interpretation of spectra and rapid time variations of type-B aurora. *Planet. Space Sci.* **27**, 169.

Hecht, J. B., Christensen, A. B. and Pranke, J. B. (1985) High resolution auroral observations of the OI (7774) and OI (8446) multiplets. *Geophys. Res. Lett.* **12**, 605.

Henriksen, K. and Veseth, L. (1987) Analysis of auroral O_2^+ first negative bands. *Can. J. Phys.* **65**, 1119.

Henriksen, K., Veseth, L., Deehr, C. S. and Smith, R. W. (1987) Neutral temperatures and emission height changes in an *E*-region aurora. *Planet. Space Sci.* **35**, 1317.

Hunten, D. M. (1955) Some photometric observations of auroral spectra. *J. atmos. terr. Phys.* **7**, 141.

Lummerzheim, D. (1987) Electron transport and optical emissions in the aurora. Ph.D. thesis, University of Alaska, Fairbanks.

McEwen, D. J. and Bryant, D. A. (1978) Optical-particle characteristics of pulsating aurora. *J. atmos. terr. Phys.* **40**, 871.

McEwen, D. J., Duncan, C. N. and Montalbetti, R. (1981) Auroral electron energies: comparisons of *in situ* measurements with spectroscopically inferred energies. *Can. J. Phys.* **59**, 1116.

Mende, S. B., Eather, R. H., Rees, M. H., Vondrak, R. R. and Robinson, R. M. (1984) Optical mapping of ionospheric conductance. *J. geophys. Res.* **89**, 1755.

Niciejewski, R. J. and Forsyth, P. A. (1988) Auroral influence on ionospheric electron content. *Can. J. Phys.* **66**, 175.

Niciejewski, R. J., Meriwether, J. W., Jr., McCormac, F. G., Hecht, J. H., Christensen, A. B., Sivjee, G. G., Strickland, D. J. Swenson, G., Mende, S. B., Vallance Jones, A., Carlson, H. C. and Valladares, C. E. (1989) Coordinated satellite and ground-based measurements of the energy characteristics of a sun-aligned arc over Søndre Strømfjord. *J. geophys. Res.* (in press).

Rees, M. H. (1963) Auroral ionization and excitation by incident energetic electrons. *Planet. Space Sci.* **11**, 1209.

Rees, M. H. and Lucke, D. (1974) Auroral electron energy derived from ratio of spectroscopic emissions. 1—Model computations. *J. geophys. Res.* **79**, 5181.

Rodulgin, V. K. (1968) On the intensity ratio 1N O_2^+ and 1PG N_2 as a function of auroral height. Results of Researches on the International Geophysical Project. *Aurora* **17**, 59.

Sawchuk, W. and Anger, C. D. (1976) Intensity ratio $I(5577)/I(3914)$ in type-B red aurora. *Planet. Space Sci.* **24**, 893.

Shemansky, D. E. and Vallance Jones, A. (1968) Type-B red aurora; the O_2^+ first negative system and the N_2 first positive system. *Planet. Space Sci.* **16**, 1115.

Vallance Jones, A. (1974) *Aurora*. D. Reidel, Dordrecht, Holland.

Vallance Jones, A. (1975) A model for the excitation of electron aurora and some applications. *Can. J. Phys.* **53**, 2267.

Vallance Jones, A. and Gattinger, R. L. (1972) Quantitative spectrospcy of the aurora. I—The spectrum of bright aurora between 7000 and 9000 Å at 7.5 Å resolution. *Can. J. Phys.* **50**, 1833.

Vallance Jones, A., Gattinger, R. L., Shih, P., Meriwether, J. W., Wickwar, V. B. and Kelly, J. (1987) Optical and radar characterizations of a short-lived event at high latitude. *J. geophys. Res.* **92**, 4575.

Vondrak, R. R. and Baron, M. J. (1976) Radar measurements of the latitudinal variation of auroral ionization. *Radio Sci.* **11**, 939.

Vondrak, R. R. and Sears, R. D. (1978) Comparison of incoherent scatter radar and photometric measurements of the energy distribution on auroral electrons. *J. geophys. Res.* **83**, 1665.